Thyroid hormone signalling in Osteoarthritis: early life events in late life disease

Bömer, N.

Chapter 6

Neo-cartilage engineered from primary chondrocytes is epigenetically similar to autologous cartilage, in contrast to using mesenchymal stem cells

N. Bomer[1,2], W. den Hollander[1], H. Suchiman[1], E. Houtman[1], R.C. Slieker[1,2], B.T. Heijmans[1,2], P.E. Slagboom[1, 2], R.G.H.H. Nelissen[3], Y.F.M. Ramos[1], I. Meulenbelt[1,*].

[1]Dept. of Molecular Epidemiology, LUMC, Leiden, The Netherlands. [2]IDEAL, [3]Dept. of Orthopaedics, LUMC, Leiden, The Netherlands.

Edited version of: Osteoarthritis and Cartilage Aug;24(8):1423-30 (2016)

Abstract

Objectives: To compare the epigenetic landscape of 3D cell models of human primary articular chondrocytes (hPACs) and human bone-marrow derived mesenchymal stem cells (hBMSCs) and their respective autologous articular cartilage.

Design: Using Illumina Infinium HumanMethylation450 BeadChip arrays, the DNA methylation landscape of the different cell sources and autologous cartilage was determined. Pathway enrichment was analyzed using DAVID.

Results: Principal Component Analysis (PCA) of methylation data revealed separate clustering of hBMSC samples. Between hBMSCs and autologous cartilage 86881 CpGs (20,2%), comprising 3034 differentially methylated regions (DMRs; $\Delta\beta>0.1$; with the same direction of effect), were significantly differentially methylated. In contrast, between hPACs and autologous cartilage only 5706 CpGs (1,33%) were differentially methylated. Of interest was the finding of the transcriptionally active, hyper-methylation of a Cartilage Intermediate Layer Protein (*CILP)* annotated DMR ($\Delta\beta=0.16$) in PAC-cartilage, corresponding to a profound decrease in *CILP* expression after *in vitro* culturing of hPACs as compared to autologous cartilage.

Conclusions: In vitro engineered neo-cartilage tissue from primary chondrocytes, hPACs, exhibits a DNA methylation landscape that is almost identical (99% similarity) to autologous cartilage, in contrast to neo-cartilage engineered from bone marrow-derived MSCs. Although hBMSCs are widely used for cartilage engineering purposes the effects of these vast differences on cartilage regeneration and long term consequences of implantation, are not known. The use of hBMSCs or hPACs for future cartilage tissue regeneration purposes should therefore be investigated in more depth in future endeavors to better understand the consequences of the differential methylome on neo-cartilage.

Introduction

Articular cartilage is a highly specialized tissue present in all synovial joints at the ends of longitudinal bones. Its main function is to facilitate protection of subchondral bone against heavy loads, while maintaining smooth locomotor function of the articular joint[1]. Emerging data show that DNA methylation of CpG dinucleotides has a prominent function in both dynamic changes in gene expression and maintaining cellular phenotypes[2-4]. DNA methylation, in which the cytosine residue in cytosine-phosphate-guanine dinucleotides (CpGs) acquires a methyl group, is known to regulate gene expression upon environmental changes such as age and disease. Loss of epigenetic control of articular chondrocytes could be one of the underlying mechanisms preceding disease onset of e.g. osteoarthritis[5]. With age and trauma, articular chondrocytes tend to undergo progressive dedifferentiation[6-8] and degeneration[9-11], resulting in degradation of the cartilage extra cellular matrix (ECM) and subsequent calcification[12], yet without effective treatment. To repair damaged cartilage, regeneration therapies have shown promising results[13-15]. Despite these successes, limitations clearly exist. The shortage of human primary articular chondrocytes (hPACs) and the dedifferentiation encountered in *in vitro* culturing are considered major hurdles. For that matter, mesenchymal stem cells (MSCs) were found to be a promising alternative as candidate cells for cartilage tissue engineering[16]. MSCs can be obtained in large quantities from e.g. adipose tissue and bone marrow and can be expanded for a number of passages without losing their ability to undergo chondrogenic differentiation[17, 18]. Unfortunately, the phenotype of MSCs in cartilage repair is unstable[19]. The expression of cartilage hypertrophy markers by MSCs undergoing chondrogenesis, raises concerns for clinical applications of MSC-based tissue engineering, since chondrocyte hypertrophy in neo-cartilage could ultimately lead to apoptosis and ossification[20, 21]. The exact molecular mechanism underlying hypertrophic differentiation is not understood and despite numerous studies about the function of single signaling pathways in hypertrophy, studies which explore comprehensive pathways in hypertrophic differentiation of MSCs and chondrocytes have not been published in recent years[22]. Moreover, these studies have, until now, not looked at the genome wide DNA methylome which is a crucial regulator of cellular identity and characterizes tissue homeostasis. Overall differences in the methylome on the tissue level are commonly reflected in differentially methylated regions (DMRs), whereas changes in methylation at single CpGs are found to mark, dynamic responses to environmental challenges but also merely stochastic differences at the individual level.[3, 23] For that matter, both changes in DMRs as well as at CpG-sites are known to modulate transcription factor binding and thereby dynamically regulating gene expression[3, 24, 25]. In this study, we examined the genome-wide DNA methylation profiles of 3D chondrogenic cultured human bone marrow-derived MSCs (hBMSCs) and hPACs, against those of the respective hip and knee autologous cartilage.

Materials and methods

Biobanking and tissue sampling

As part of the ongoing RAAK study, ethical approval was obtained from the medical ethics committee of the LUMC (P08.239) and informed consent was obtained from all participants. Participant details are listed in Table S1. Tissue sampling was performed as described before[26]. In short, within 2 hours following surgery, cartilage was washed extensively with phosphate buffered saline to decrease the risk of contamination with blood. Macroscopically unaffected cartilage was sampled from patients who underwent a total joint replacement due to primary OA of either knee (N=6) or hip (N=5). During collection with a scalpel, care was taken to avoid contamination with bone or synovium. Collected cartilage was snap frozen in liquid nitrogen and stored at -80°C prior to RNA and DNA extraction.

Cell isolation and culture

hBMSCs were isolated from hip joints of 4 OA patients who underwent total hip arthroplasty as result of end stage OA as part of the RAAK study. Proliferation for the quantitative expansion of cells, formation of 3D pellet cultures and subsequent chondrogenic differentiation were performed as described before[27]. In short, hBMSCs were expanded for 5 passages before the formation of pellet cultures in 15 ml polypropylene conical tubes. Pellet cultures were harvested for RNA and DNA isolation purposes at time points 14, 21, 35 and 49 days after the start of differentiation. Micromasses were harvested from 14 days onwards, earlier results showed that around this time point, the cells in the micromass-cultures are differentiated towards chondrocytes, capable of depositing cartilage-like extracellular matrix[27] (Figure S1). For every time point, per donor, two separately grown 3D pellet-cultures were pooled as 1 sample before DNA isolation, resulting in 4 independent samples per timepoint.

hPACs were isolated from cartilage derived from four OA patients who underwent total joint arthroplasty of the knee (RAAK study). Macroscopically unaffected cartilage tissue was incubated overnight in DMEM (high glucose; Gibco, Bleiswijk, The Netherlands) supplemented with 10% fetal bovine serum (FBS; Gibco), antibiotics (100 U/ml penicillin, 100 µg/ml streptomycin; Gibco) and 2 mg/ml collagenase type I at 37 °C in a humidified 5% CO2 / 95% atmosphere. Subsequently, primary chondrocytes were resuspended and filtered through a 100 µm mesh to remove undigested cartilage fragments and extracellular matrix debris. Cells were expanded at 37 °C in a humidified 5% CO_2 / 95% atmosphere in DMEM supplemented with 10% FBS, penicillin (100 units/mL), streptomycin (100 units/mL) and 0.5 ng/ml FGF-2 (PeproTech, Heerhugowaard, The Netherlands) for 2 passages. 3D pellets were formed using centrifugal forces (1200 rpm; 5 min) on 2.5 x 10^5 cells in 15 ml polypropylene conical tubes. Chondrogenesis was initiated in 1 ml serum-free chondrogenic differentiation medium (DMEM, supplemented with Ascorbic acid (50 µg/ml; Sigma-Aldrich; Zwijndrecht, The Netherlands), L-Proline (40 µg/ml; Sigma-Aldrich), Sodium Puryvate (100 µg/ml; Sigma-Aldrich), Dexamethasone (0.1 µM; Sigma-Aldrich), ITS+ (Sigma-Aldrich), antibiotics, and TGF-β1 (10 ng/ml; PeproTech)). Medium was

changed every 3-4 days. Pellet cultures were harvested for RNA and DNA isolation purposes at time points 0, 4, 7, 14 and 21 days after the start of differentiation. 0 days hPACs were included as starting point of harvesting, since these cells are already fully differentiated chondrocytes, capable of depositing cartilage-ECM and therefore more or less represent the state in which the 14 days differentiated hBM-MSCs are. Based on 3D micromass culture experiments using ATDC5 cells[28], we decided to use these timepoints (7, 14 and 21 days) for our experiments, with the addition of an early timepoint (4 days) (Figure S1). For every time point, per donor, two separately grown 3D pellet-cultures were pooled as 1 sample before DNA isolation, resulting in 4 independent samples per timepoint.

DNA isolation

Snap frozen articular cartilage was powderized using a Mixer Mill 200 (Retsch, Germany) with continuous liquid nitrogen cooling. DNA was isolated using the Wizard Genomic DNA Purification kit (Promega, Madison, WI, USA) according to the manufacturer's protocol.

Methylation arrays

DNA was bisulphite treated using the EZ DNA Methylation kit (Zymo Research Corp, Irvine, CA, USA). DNA methylation was assessed using Infinium HumanMethylation450 BeadChips (Illumina, San Diego, CA, USA). All methylation values are reported as fractions between 0 and 1, commonly known as the β value. Samples were randomly dispersed, while sample pairs were assured to be on the same chip. Raw IDAT files were applied in R statistical language using the *minfi* package[29] and were subjected to standard quality control steps, including bisulphite conversion rate and outlier detection. Ambiguously mapping probes were removed prior to normalization[30]. Next, probes of which over 1% of the samples showed a detection P-value over 0.05 were removed. Probes for which either the green or red channel showed an intensity of 0 were removed as well. In total 32693 probes were removed prior to normalization. Visual inspection of sample clustering was done to detect outliers prior to normalization. Background correction and raw signal normalization (quantile) were performed using the *lumi* package[31], separately for both colour channels. The BMIQ formula was used for correcting probe design bias in the 450k DNA methylation data[32]. Probe level intensities were quantile normalized across samples prior to calculation of the β-values. Using the R package IlluminaHumanMethylation450k.db, Illumina identifiers were mapped to the hg19 genome build[33]. CpGs with P-val ≤0.05 after Bonferroni correction for multiple testing were considered significant.

Principal component analysis and statistical analyses

Principal Component Analysis (PCA) was performed in R on the DNA methylation data to identify putative clusters using an unbiased method. Further statistical analyses were carried out using the *lme4* package. All analyses were performed using linear mixed models (LMMs) and were executed including all timepoints per cell-type. Furthermore, they contained a random effect for patient ID to account for putative correlations and inherent individual differences. Methylation measurements are reported as β-values, reflecting

the fraction of methylation between 0 and 1. Differentially methylated regions (DMRs), stratified for hypo- and hyper-methylated CpGs, were defined by three consecutive significantly differentially methylated CpGs by at least 0.1 |Δβ| and at most 1000 base pairs apart, while allowing for a maximum of three non-significant CpGs[3]. A single DMR can contain CpGs annotated to different genes, therefore, pathway enrichment analysis was performed on all official gene symbols annotated to a DMR by its CpGs. Enrichment analyses were performed using the online annotation tool DAVID[34]. Pathways with P-val ≤0.05 after Bonferroni correction for multiple testing were considered significant.

Expression data and t-CpGs

Normalized expression data of articular cartilage from the RAAK study were processed and normalized as described previously (GSE57218)[26]. Normalized methylation data of the articular cartilage samples overlapping the samples used for expression were processed and normalized as described previously[35]. In short, for the 13277 probes (covering 9838 unique genes) that were expressed to detectable extent in articular cartilage, the association with DNA methylation of proximal CpGs was determined. DNA methylation data of CpGs within 10kb of annotated genes was correlated to respective gene expression data of articular cartilage. After multiple testing correction for the number of CpGs for each individual gene, 3748 CpGs were observed that significantly correlated with proximal gene expression, hereafter indicated as transcriptionally active CpGs (t-CpGs)[35].

RNA isolation and RT-qPCR and statistical analysis

Isolation of RNA was performed as described previously[27]. RNA quantity was assessed using a nanodrop spectrophotometer (Thermo Fisher Scientific Inc., Wilmington, USA). 500 ng of total RNA was processed with the First Strand cDNA Synthesis Kit according to the manufacturer's protocol (Roche Applied Science, Almere, The Netherlands), upon which cDNA was diluted 5 times. RT-qPCR measurements were performed on the Roche Lightcycler 480 II, using Fast Start Sybr Green Master reaction mix according to the manufacturer's protocol (Roche Applied Science). Relative gene expressions of the Roche Lightcycler 480 II data were calculated by using the $2^{-\Delta\Delta Ct}$ method, in which Ct indicates the fractional cycle number where the fluorescent signal reaches detection threshold[36]. Primer sequences used are listed in Supplementary Table S2. The housekeeping gene, glyceraldehyde 3-phosphate dehydrogenase (*GAPDH*) was used as a single reference gene for qPCR[37, 38]. The paired-student T-test was used to calculate the significance of differences in expression between the samples of different origins. All P-values < 0.05 were considered statistically significant.

Results

Principal component analyses (PCA) reveals distinct differences in the epigenetic landscape

Genome wide DNA methylation profiling was performed in all samples, consisting of 3D

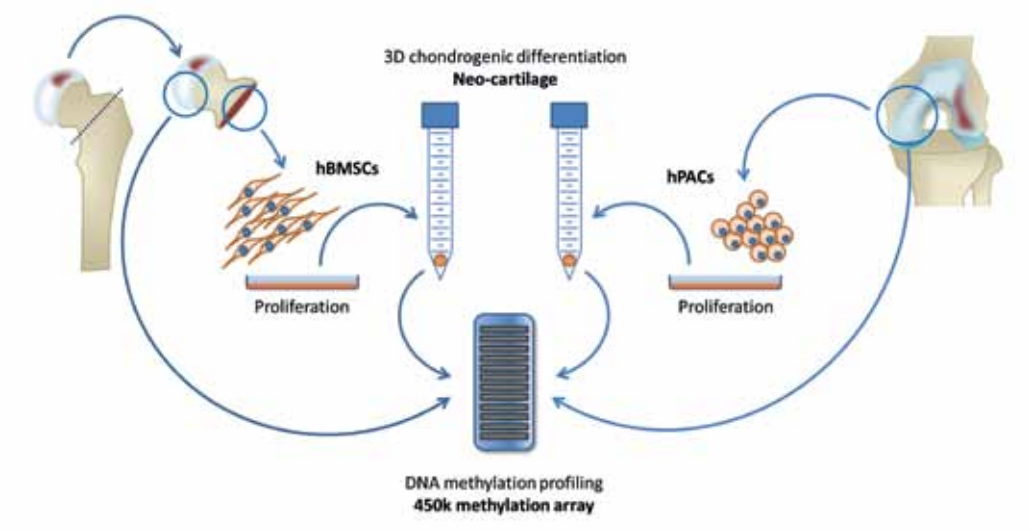

Figure 1: Graphical representation of the study-design.
Human bone marrow derived mesenchymal stem cells (hBMSCs) were isolated from hip joints of OA patients who underwent total hip arthroplasty as result of end stage OA as part of the RAAK study. Primary articular chondrocytes (hPACs) were isolated from macroscopically unaffected cartilage derived from four OA patients who underwent total joint arthroplasty of the knee (RAAK study). Subsequent the cells are proliferated for the expansion of cell-numbers. Next, 3D pellet cultures are formed and chondrogenic differentiation is commenced to engineer hBMSCs-derived neo-cartilage (MSC-cartilage) and hPACs-derived neo-cartilage (PAC-cartilage). Neo-cartilage is isolated for DNA isolation at time points of 14, 21, 35 and 49 days for MSC-cartilage and 0, 4, 7, 14 and 21 days for PAC-cartilage. The genome-wide DNA methylation profiles of MSC-cartilage and PAC-cartilage was compared against those of the respective hip and knee autologous cartilage using Illumina 450k methylation arrays.

chondrogenic cultured hBMSCs derived neo-cartilage (MSC-cartilage; N=4) and hPACs derived neo-cartilage (PAC-cartilage; N=4), and macroscopically unaffected articular cartilage derived from the 4 knee and 4 hip joints from which the cells originated (autologous), as well as 3 additional independent joints (2 knees and 1 hip) (Figure 1). By means of PCA we observed two distinct clusters of samples, being the knee, hip and PAC-cartilage samples together (cluster 1) and the MSC-cartilage separate (cluster 2) on the first component (Figure 2A) indicating that cells in MSC-cartilage samples have a distinct DNA methylation profile compared to autologous cartilage and PAC-cartilage (Figure 2B). On the second PCA component separation of the samples was observed between autologous- and PAC-cartilage (Figure 2A).

The epigenetic landscape of MSC-cartilage is very distinct to autologous cartilage

To elucidate the DNA methylation differences driving the distinct clustering of MSC-cartilage in the PCA, we assessed which CpG-sites were differentially methylated between MSC-cartilage and autologous cartilage (both hip and knee cartilage). We selected CpGs

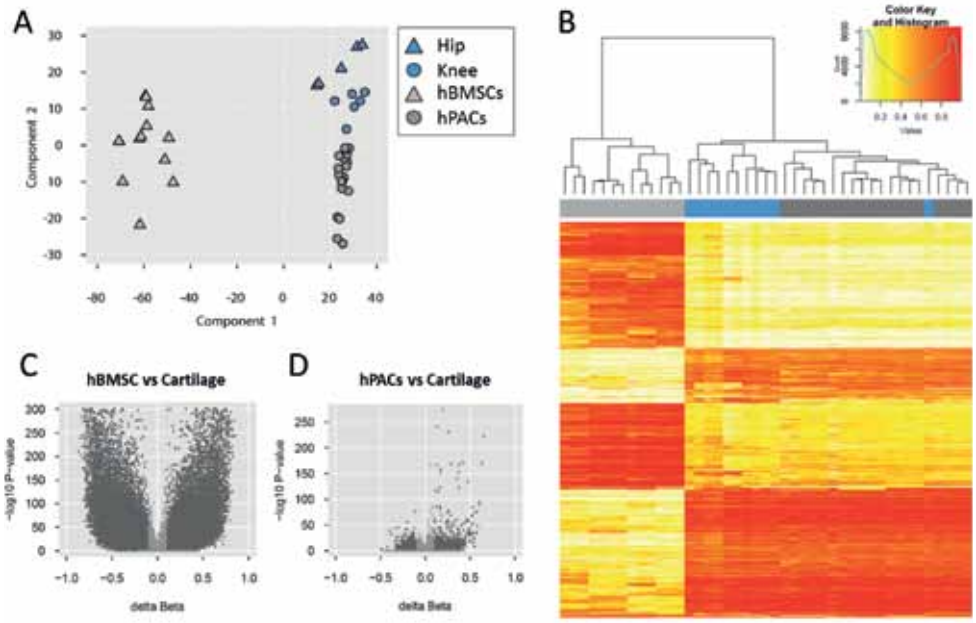

Figure 2. Graphical data representations.
(A) Principle Component Analysis (PCA) displaying the first two components (component 1 (x-axis) and component 2 (y-axis)). (B) Heatmap constructed from the 10000 CpGs (y-axis) that showed the largest variation (Standard Deviation) over the samples (x-axis). Samples are hierarchically clustered (dendogram on the top), showing two distinct clusters: hBMSCs (light grey) and cartilage (blue) and hPACs (dark grey) together. (C) Volcano-plot of all CpGs after QC (438750) for the comparison of methylation status in hBMSCs against preserved cartilage. CpGs that reach the threshold (P<0.05 & Δβ>0.1) are printed dark grey, CpGs that do not reach the threshold are printed in light grey. (D) Volcano-plot of all CpGs after QC (438750) for the comparison of methylation status in hPACs against preserved cartilage.

that showed significant differential methylation (P<0.05; after adjustment for multiple testing according to Bonferroni) by at least 10% methylation difference (Δβ), between MSC-cartilage and paired autologous cartilage (86881 CpGs) independent of the time point of harvest (Figure 2C; Table S3). To prioritize on DMRs, we applied a sliding window algorithm[3] on the differentially methylated CpGs, to distinguish inherent MSC-cartilage differences in the methylation data (DMRs) from possible environmental, stochastic or individual CpG differences (default setting: DMR ≥ 3CpGs). A total of 5884 DMRs were identified, 2855 hypo-methylated DMRs in MSC-cartilage compared to autologous cartilage, and 3029 hyper-methylated DMRs. To be able to perform pathway analyses with DAVID, which allows enrichment analyses for 3000 genes, we raised the threshold for DMR calling from 3 to 4 CpGs. This resulted in 3034 DMRs (1504 hypo-methylated; 1530 hyper-methylated), comprising 16820 CpGs, annotated to 3107 unique transcripts (Table S4), coding for 2575 unique proteins.
Overall pathway enrichment using DAVID revealed enrichment clusters for pathways

Tabel 1. Summary of Annotation clustering results from DAVID analysis of unique gene symbols annotated to the DMRs in hBMSCs

	Category	Term	Count	Bonferroni
Annotation Cluster 1 *Enrichment Score: 13,53*	INTERPRO	IPR001356:Homeobox	72	1,88E-10
Annotation Cluster 2 *Enrichment Score: 8,07*	GOTERM_BP_FAT	GO:0048598~embryonic morphogenesis	92	1,35E-12
Annotation Cluster 3 *Enrichment Score: 7,52*	GOTERM_BP_FAT	GO:0007389~pattern specification process	67	0,000071
Annotation Cluster 5 *Enrichment Score: 7,13*	GOTERM_BP_FAT	GO:0060173~limb development	35	0,00014
Annotation Cluster 7 *Enrichment Score: 5,51*	GOTERM_BP_FAT	GO:0048705~skeletal system morphogenesis	34	0,0045
Annotation Cluster 8 *Enrichment Score: 4,63*	GOTERM_BP_FAT	GO:0060429~epithelium development	57	0,00091
Annotation Cluster 18 *Enrichment Score: 2,73*	GOTERM_BP_FAT	GO:0030182~neuron differentiation	89	0,0087

involved in various developmental and transcription regulation processes (GO- and INTERPRO-terms). Amongst others, processes known to be involved in skeletal development and morphogenesis, like: homeobox, embryonic morphogenesis, pattern specification process, limb development and skeletal system morphogenesis (Table 1). But also pathways less recognizable for cartilage development, such as neuron differentiation and epithelium development (Table 1).

Notably, DMRs of the counted genes of Table 1, appeared to be marked by large methylation differences ($\Delta\beta>0.5$), as such potentially affecting respective transcriptional activity[3, 25, 35]. These are genes known to be important in de early development of the skeleton (e.g. *LRP5, COL11A2, MSX1, GLI3, WNT5A* and *TWIST1*), but also neuronal development (*ISL1, DLX2, IRX3* and *DLX1*). To assess the potential transcriptional consequences of these CpG sites, we examined correlation between methylation and transcription of these genes (*in silico*) in a previously assessed dataset of articular cartilage[35]. Methylation of N= 65 out of N= 583 CpG sites appear to show strong correlation with expression in articular cartilage (Figure 3A-E)[35].

The epigenetic landscape of PAC-cartilage is very similar to analogous cartilage

To identify which genes/processes are epigenetically differently regulated in hPACs proliferated in 2D and cultured under 3D chondrogenic conditions (PAC-cartilage), as com-

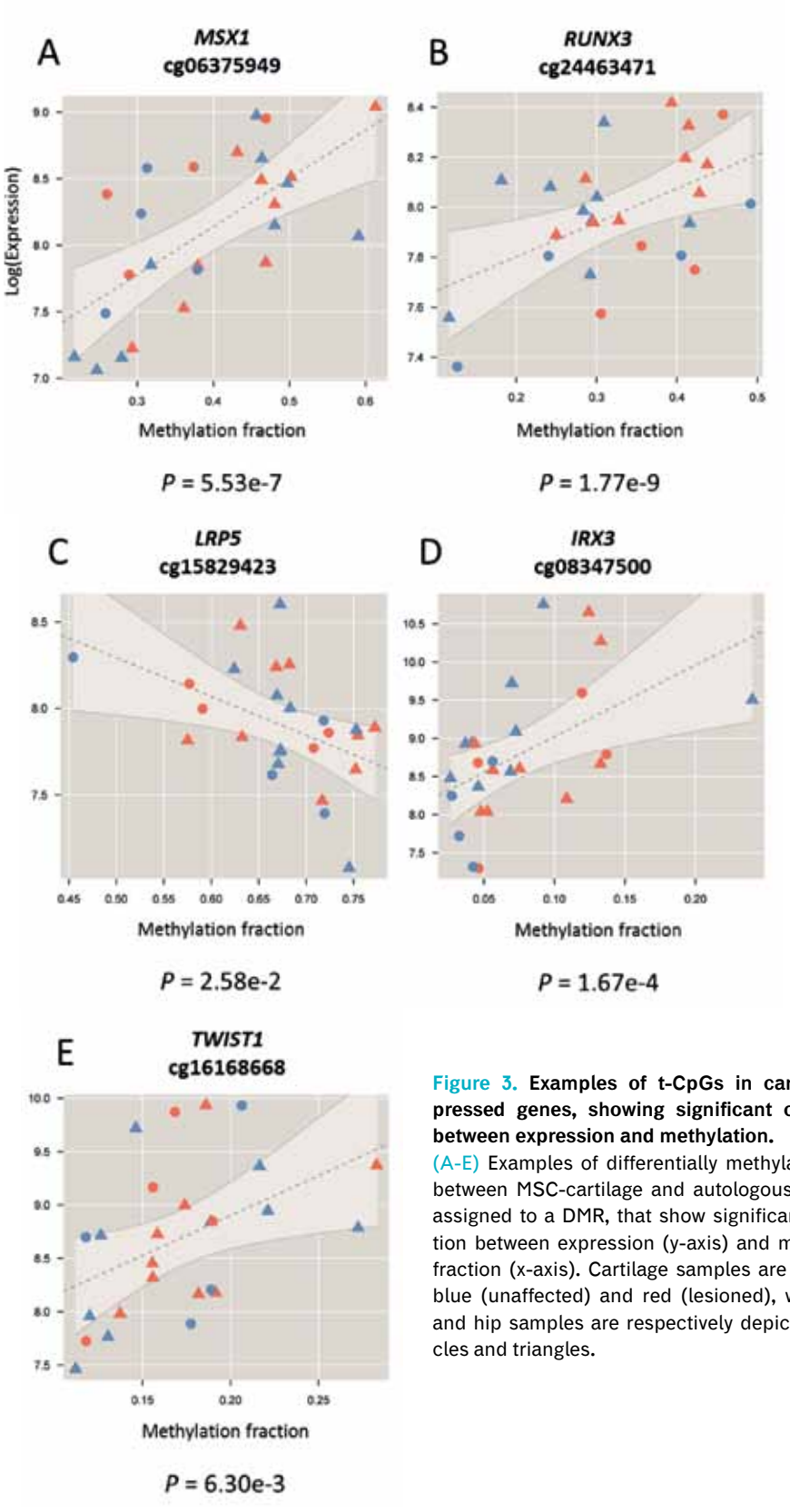

Figure 3. Examples of t-CpGs in cartilage expressed genes, showing significant correlation between expression and methylation.
(A-E) Examples of differentially methylated CpGs between MSC-cartilage and autologous cartilage, assigned to a DMR, that show significant correlation between expression (y-axis) and methylation fraction (x-axis). Cartilage samples are printed in blue (unaffected) and red (lesioned), while knee and hip samples are respectively depicted as circles and triangles.

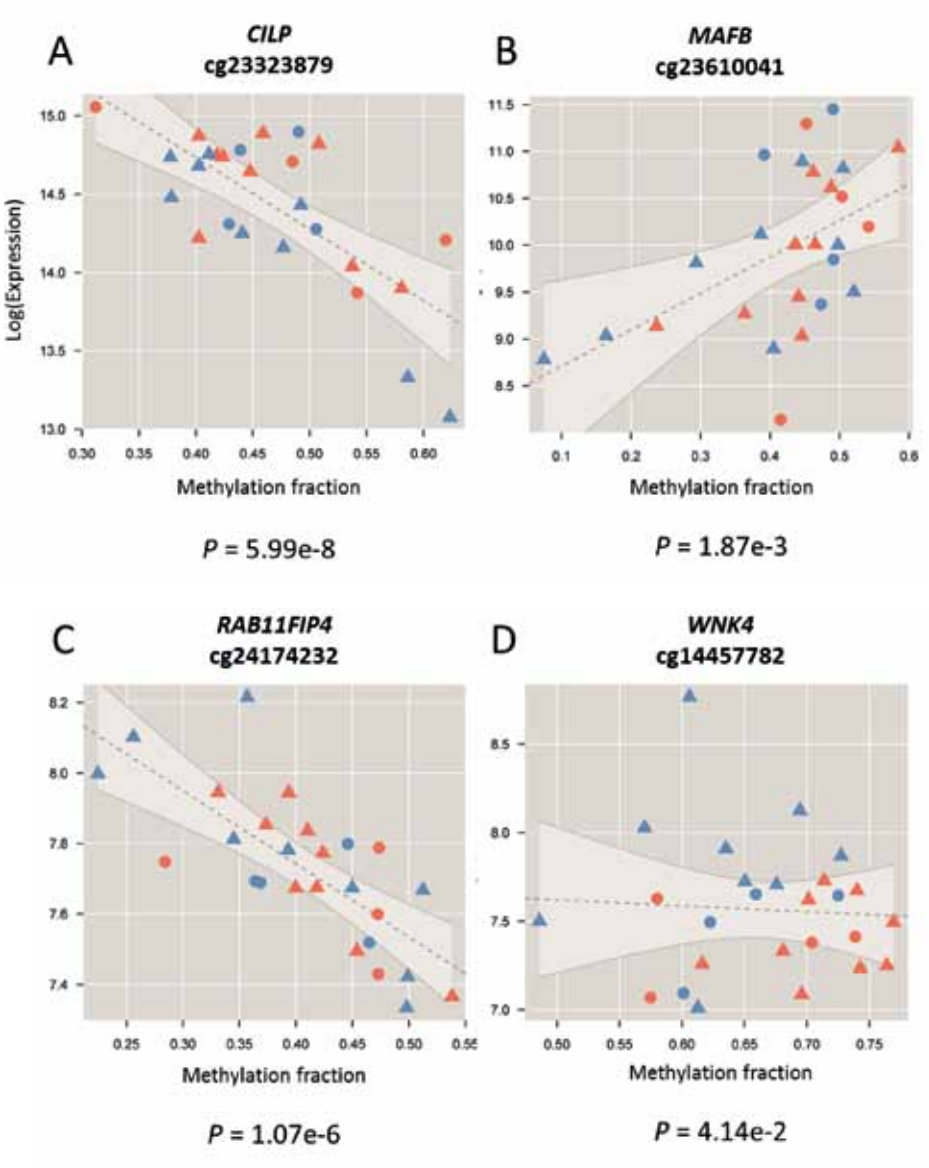

Figure 4. Examples of t-CpGs in cartilage expressed genes, showing significant correlation between expression and methylation.

(A-D) Examples of differentially methylated CpGs between PAC-cartilage and autologous cartilage, assigned to a DMR, that show significant correlation between expression (y-axis) and methylation fraction (x-axis). Cartilage samples are printed in blue (unaffected) and red (lesioned), while knee and hip samples are respectively depicted as circles and triangles.

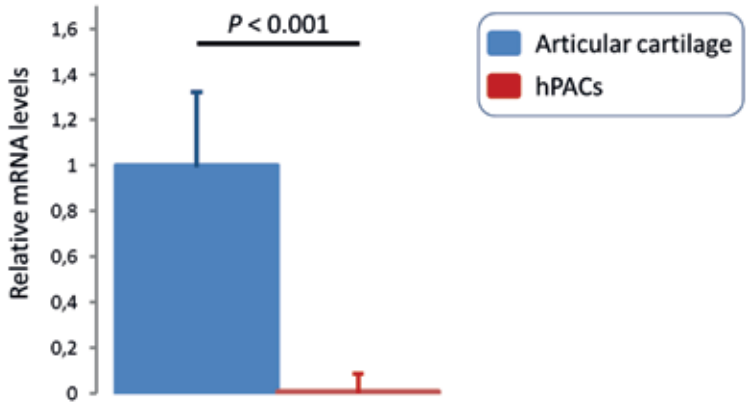

Figure 5. RT-qPCR analysis of *CILP* expression in in vitro cultured hPACs and autologous articular cartilage.
CILP mRNA levels were found down regulated 97–fold. Data is presented as the mean+SD of RT-qPCR triplicates and relative to articular cartilage expression.

pared to the chondrocytes directly isolated from the articular cartilage for DNA extraction (Figure 1), we identified CpGs that showed significant differential methylation ($P<0.05$ & $\Delta\beta>0.1$) between PAC-cartilage and the paired autologous, macroscopically unaffected, cartilage. As of such, we observed 5706 differentially methylated CpGs (1,33% of total CpGs) (Figure 2D; Table S5). Here, no significant differences in methylation where obtained as a consequence of timepoint of harvest. From the differential methylated CpGs, a total of 62 DMRs (45 hyper- and 17 hypo-methylated), comprising of 215 CpGs were called (Table S6). Because a single DMR can contain CpGs annotated to different genes these were mapped to 71 unique transcripts.

Pathway enrichment of all transcripts residing in these DMRs did not result in significant hits. Nevertheless, multiple DMRs were annotated to genes known to be involved in ECM composition (*CILP, COL9A3, SPON2* and *FBLN2*) and endochondral ossification (*GDF7*). Of these 8 CpGs (Table S7) were identified as t-CpG in the articular cartilage dataset as outlined above[35] and were annotated to 4 genes (*CILP, MAFB, RAB11FIP4* and *WNK4*) (Figure 4A-D). Except for *MAFB*, a negative correlation between DNA methylation and expression was observed.

Given the fact that *CILP* is amongst the highest expressed genes in articular cartilage[26], yet contains hyper-methylated t-CpG sites [35] in a DMR in PAC-cartilage as compared to autologous cartilage, we examined *CILP* expression levels in *in vitro* proliferated hPACs and analogous knee-cartilage tissue. A 97-fold decrease in expression in hPACs as compared to autologous cartilage (Figure 5) was observed.

Discussion

Here we show that chondrogenic 3D cultured MSC-cartilage exhibit an entirely distinct epigenetic signature as compared to 3D cultured PAC-cartilage and the respective autologous hip and knee cartilage. The epigenetic profile of PAC-cartilage, however, resembles 99% of that of the autologous cartilage from which the cells were isolated. This indicates that the use of hPACs for tissue engineering purposes could be favored above hBMSCs, despite the encountered difficulties with *in vitro* culturing, since the long term effects of the differential methylome are not known. In order to overcome this hurdle, the option of constructing neo-cartilage from hPACs, or even hPAC-dervived iPS cells, instead of using hBMSCs as a cell source should be investigated[39].

Conversely, the effect of *ex vivo* culturing of hPACs showed only 1,33% of CpGs (5706) on the 450k array to be significant differentially methylated ($P<0.05$ & $\Delta\beta>0.1$). The resulting 62 DMRs were, amongst others, located near genes known to be involved in ECM homeostasis (*CILP, COL9A3, SPON2* and *FBLN2*) and endochondral ossification (*GDF7*). Furthermore, DMRs in 4 genes, *CILP, MAFB, RAB11FIP4* and *WNK4*, were identified to harbor t-CpGs that exhibit a significant correlation between DNA methylation and expression in articular cartilage[35]. We assessed the presence of t-CpGs, since these are believed to imply the direct relationship between the observed methylation and expression in articular cartilage. Nonetheless, our data shows that although methylation profiles at DMRs are highly tissue-type specific, they do not necessarily correlate to gene expression, as only a minority of DMRs appear to be associated with cartilage specific gene expression differences. Consequently, most of these CpG-methylation differences may therefore not be detected as t-CpGs in the study of *den Hollander et al.*[35] or vice versa.

The consistent positive correlation between methylation and expression, as seen for 4 out of 5 genes in figure 3, may not comply with the conventional inverse relation between CpG methylation and gene expression. However, in recent genome-wide approaches, it has been recognised that this conventional relation primarily holds among CpG dinucleotides residing in CpG islands and proximal promoters, whereas gene body and distal enhancer methylation, has been shown to correlate in either direction with gene expression[40-42]. For example, a recent study investigating the transcriptional associations of osteoarthritis-mediated loss of epigenetic control in articular cartilage showed that of 9,838 transcribed genes in articular cartilage, 2,324 correlated with the methylation status of 3,748 transcriptionally active CpG; both negative (n = 1,741) and positive (n = 2,007) correlations were observed[35].

Of particular interest was the finding of the transcriptionally active, hyper-methylation of a Cartilage Intermediate Layer Protein (*CILP)* annotated DMR ($\Delta\beta=0.16$) in PAC-cartilage, that corresponded to a profound decrease in *CILP* expression after *in vitro* culturing of hPACs as compared to autologous cartilage. Such a reduced expression of *CILP* during *in vitro* chondrogenesis of hPACs, is thought to increase the necessary *TGF-β1*-induced *COL2A1* and *ACAN* expression; the key building blocks of articular cartilage and the formation of proper ECM. On the other hand, the extreme high levels of *CILP* expression in autologous articular cartilage[26], induced by *BMP2*[43], likely mark the relative

senescent state in which chondrocytes reside in healthy cartilage ECM. Although there is only a few percentage difference in the epigenetic landscapes of autologous cartilage and hPACs, these differences are likely markers for the dedifferentiation process which occurs when hPACs are brought into culture. Therefore we believe that the correlations as seen for CILP in this study, represent a transcriptional marker that is likely necessary for the formation of ex vivo neo-cartilage formation. As such, the effect of altered CILP expression on TGF-B1 induced anabolic processes and the corresponding consequence on integrity of the cartilage homeostasis warrants more in depth exploration, particularly for tissue regeneration purposes."

To investigate whether the differences in the epigenetic landscape, observed between hBMSCs- and hPACs-derived and autologous cartilage, where actually driven by changes in the epigenetic landscape that occur during chondrogenesis both in MSC and PACs, we performed an analysis identifying CpGs with significantly methylation differences with time course (t = 14, 21, 35 and 49 days, and t= 0, 4, 7, 14 and 21 days respectively). As depicted in Table S8, (1116 CpGs in hBMSCs) & Table S9 (58 CpGs in hPACs), however, these CpG sites only slightly overlap with the differences in the epigenetic landscape observed between hBMSCs and hPACs derived and autologous cartilage shown in Tables S3 (267 CpGs for hBMSCs) & S5 (2 CpGs for hPACs). Ergo, it does not explain the large difference comparing autologous cartilage against hBMSCs and hPACs. It could be pointed out that the chondrogenically differentiated hBMSCs represent a mixed phenotype and that the differentiation is likely less advanced than the already differentiated hPACs. Nonetheless, we started to include hBMSC-derived micromasses from 14 days onwards, since our experience[27] showed that around this time point, the cells in the micromass cultures are differentiated in such a way, that they start producing cartilage-like extracellular matrix. At the more advanced timepoints of chondrogenesis (35 & 49 days of MSC-cartilage and 14 & 21 days of PAC-cartilage), the micromass cultures (deposited glycosaminoglycans) are optically similar in appearance (Figure S1) and stratified analyses of these late timepoints were found to display comparable epigenetic differences towards autologous cartilage as in the initial comparison.

Since the differences in DNA methylation between MSC-cartilage and autologous cartilage are substantial, the question should be raised whether the use of hBMSCs for tissue regeneration purposes is eligible. For example, DMRs that harbor CpGs with large methylation differences were found to be annotated to genes that are not only important for development, but are also associated with cancer pathways (*RUNX3, TWIST1, GLI3, WNT5A, TP63* and *STAT3*)[44-49]. The alternative epigenetic regulation found in MSC-cartilage is therefore difficult to explain and we do not yet know what the long term consequences are of implanting regenerated tissue that is epigenetically very distinct from its target tissue. It was reviewed recently, that results from pre-clinical studies suggest that the MSCs injected for regeneration purposes served an directive role as opposed to supplying the direct building blocks[50].

Given that after *in vitro* proliferation for 2 passages and 3D chondrogenic culturing, the methylome of hPACs still resembles almost 99% of that of autologous cartilage, the utilization of hPACs, instead of hBMSCs for tissue regeneration purposes, should be seri-

ously considered. In light of the increasing proof of the generic presence of adult tissue-specific stem cells[51], it could also be hypothesized that by isolating and proliferating primary chondrocytes, we enrich the cell culture for highly specialized, unipotent adult cartilage stem cells. This cell population could in theory be, epigenetically, perfectly programmed for chondrogenesis purposes. A first step to substantiate this hypothesis is to search for such cartilage resident adult stem cells

Here we have shown that, based on genome wide DNA methylation profiles, neo-cartilage engineered from hPACs is almost identical to its autologous donor. In contrast, neo-cartilage engineered from hBMSCs, has a distinct DNA methylation profile as compared to autologous cartilage. Many transcription factors important for general development and morphogenesis were shown to harbor DMRs. So, although hBMSCs are widely used for cartilage engineering purposes, the effects of these vast methylation differences on cartilage regeneration and long term consequences of implantation, are not known. Therefore, the choice of cell source for future cartilage tissue regeneration purposes should be investigated in future endeavors.

Acknowledgements

We acknowledge support by IDEAL, funded by the European Union's Seventh Framework Program (FP7/2007-2011) under grant agreement no. 259679. Furthermore, this work was supported by the Dutch Arthritis Association. The funders had no role in study design, data collection and analysis, decision to publish or preparation of the manuscript.

Competing interest

The authors declare no competing financial, personal, or professional interests.

Author contributions

Conceived and designed the experiments: NB, IM.
Performed the experiments: NB; HS; EH; YR
Acquisition of material and data: NB, WH, RS, HS, RN, YR.
Preparation of the manuscript: NB, IM.
Critical reviewing and approval of the manuscript: all authors.

Supplemental Data

http://www.oarsijournal.com/article/S1063-4584(16)01070-0/addons

Reference List

1 Hosseini SM, Wu Y, Ito K, van Donkelaar CC. The importance of superficial collagen fibrils for the function of articular cartilage. *Biomech Model Mechanobiol* 2014;**13**:41-51.

2 Jaenisch R, Bird A. Epigenetic regulation of gene expression: how the genome integrates intrinsic and environmental signals. *Nat Genet* 2003;**33 Suppl**:245-54.

3 Slieker RC, Bos SD, Goeman JJ, Bovee JV, Talens RP, van der Breggen R, *et al.* Identification and systematic annotation of tissue-specific differentially methylated regions using the Illumina 450k array. *Epigenetics Chromatin* 2013;**6**:26.

4 Laurent L, Wong E, Li G, Huynh T, Tsirigos A, Ong CT, *et al.* Dynamic changes in the human methylome during differentiation. *Genome Res* 2010;**20**:320-31.

5 den Hollander W, Meulenbelt I. DNA methylation in Osteoarthritis. Current Genomics 16[6], 419-426. 2015.

6 Aigner T, Dudhia J. Phenotypic modulation of chondrocytes as a potential therapeutic target in osteoarthritis: a hypothesis. *Ann Rheum Dis* 1997;**56**:287-91.

7 Facchini A, Borzi RM, Olivotto E, Platano D, Pagani S, Cetrullo S, *et al.* Role of polyamines in hypertrophy and terminal differentiation of osteoarthritic chondrocytes. *Amino Acids* 2012;**42**:667-78.

8 Sun MM-G, Beier F. Chondrocyte hypertrophy in skeletal development, growth, and disease. *Birth Defect Res C* 2014;**102**:74-82.

9 Musumeci G, Aiello FC, Szychlinska MA, Di Rosa M, Castrogiovanni P, Mobasheri A. Osteoarthritis in the XXIst Century: Risk Factors and Behaviours that Influence Disease Onset and Progression. Int.J.Mol.Sci. 16, 6093-6112. 2015.

10 Lotz M, Loeser RF. Effects of aging on articular cartilage homeostasis. *Bone* 2012;**51**:241-8.

11 Guilak F. Biomechanical factors in osteoarthritis. *Best Practice & Research Clinical Rheumatology* 2011;**25**:815-23.

12 Dreier R. Hypertrophic differentiation of chondrocytes in osteoarthritis: the developmental aspect of degenerative joint disorders. *Arthritis Research & Therapy* 2010;**12**:216.

13 Ham O, Lee CY, Kim R, Lee J, Oh S, Lee MY, et al. Therapeutic Potential of Differentiated Mesenchymal Stem Cells for Treatment of Osteoarthritis. 16, 14961-14978. 2015. Int. J. Mol. Sci.

14 Alford JW, Cole BJ. Cartilage Restoration, Part 1: Basic Science, Historical Perspective, Patient Evaluation, and Treatment Options. *The American Journal of Sports Medicine* 2005;**33**:295-306.

15 Alford JW, Cole BJ. Cartilage Restoration, Part 2: Techniques, Outcomes, and Future Directions. *The American Journal of Sports Medicine* 2005;**33**:443-60.

16 Nejadnik H, Hui JH, Feng Choong EP, Tai BC, Lee EH. Autologous Bone MarrowGÇôDerived Mesenchymal Stem Cells Versus Autologous Chondrocyte Implantation: An Observational Cohort Study. *The American Journal of Sports Medicine* 2010;**38**:1110-6.

17 Perdisa F, Gosty+äska N, Roffi A, Filardo G, Marcacci M, Kon E. Adipose-Derived Mesenchymal Stem Cells for the Treatment of Articular Cartilage: A Systematic Review on Preclinical and Clinical Evidence. *Stem Cells Int* 2015;**2015**:597652.

18 Gnecchi M, Melo L. Bone Marrow-Derived Mesenchymal Stem Cells: Isolation, Expansion, Characterization, Viral Transduction, and Production of Conditioned Medium. In: Audet J, Stanford W, eds. *Stem Cells in Regenerative Medicine*. 482 ed. Humana Press 2009:281-94.

19 Sekiya I, Vuoristo JT, Larson BL, Prockop DJ. In vitro cartilage formation by human adult stem cells from bone marrow stroma defines the sequence of cellular and molecular events during chondrogenesis. *Proceedings of the National Academy of Sciences* 2002;**99**:4397-402.

20 Mueller MB, Tuan RS. Functional characterization of hypertrophy in chondrogenesis of human mesenchymal stem cells. *Arthritis Rheum* 2008;**58**:1377-88.

21 Gu J, Lu Y, Li F, Qiao L, Wang Q, Li N, *et al.* Identification and characterization of the novel Col10a1 regulatory mechanism during chondrocyte hypertrophic differentiation. *Cell Death Dis* 2014;**5**:e1469.

22 Zhong L, Huang X, Karperien M, Post JN. The Regulatory Role of Signaling Crosstalk in Hypertrophy of MSCs and Human Articular Chondrocytes. 16, 19225-19247. 2015. Int. J. Mol. Sci.

23 Rakyan VK, Down TA, Thorne NP, Flicek P, Kulesha E, Graf S, *et al.* An integrated resource for genome-wide identification and analysis of human tissue-specific differentially methylated regions (tDMRs). *Genome Res* 2008;**18**:1518-29.

24 Huang CZ, Yu T, Chen QK. DNA Methylation Dynamics During Differentiation, Proliferation, and Tumorigenesis in the Intestinal Tract. *Stem Cells and Development* 2015.

25 den Hollander W, Ramos YF, Bos SD, Bomer N, van der Breggen R, Lakenberg N, *et al.* Knee and hip articular cartilage have distinct epigenomic landscapes: implications for future cartilage regeneration approaches. *Ann Rheum Dis* 2014;**73**:2208-12.

26 Ramos YF, den HW, Bovee JV, Bomer N, van der Breggen R, Lakenberg N, *et al.* Genes Involved in the Osteoarthritis Process Identified through Genome Wide Expression Analysis in Articular Cartilage; the RAAK Study. *PLoS ONE* 2014;**9**:e103056.

27 Bomer N, den Hollander W, Ramos YF, Bos SD, van der Breggen R, Lakenberg N, *et al.* Underlying molecular mechanisms of DIO2 susceptibility in symptomatic osteoarthritis. *Ann Rheum Dis* 2015;**74**:1571-9.

28 Lodewyckx L, Cailotto Fdr, Thysen S, Luyten FP, Lories RJ. Tight regulation of wingless-type signaling in the articular cartilage - subchondral bone biomechanical unit: transcriptomics in Frzb-knockout mice. *Arthritis Research & Therapy* 2012;**14**:1-18.

29 Aryee MJ, Jaffe AE, Corrada-Bravo H, Ladd-Acosta C, Feinberg AP, Hansen KD, *et al.* Minfi: a flexible and comprehensive Bioconductor package for the analysis of Infinium DNA methylation microarrays. *Bioinformatics* 2014.

30 Chen YA, Lemire M, Choufani S, Butcher DT, Grafodatskaya D, Zanke BW, *et al.* Discovery of cross-reactive probes and polymorphic CpGs in the Illumina Infinium HumanMethylation450 microarray. *Epigenetics* 2013;**8**:203-9.

31 Du P, Kibbe WA, Lin SM. lumi: a pipeline for processing Illumina microarray. *Bioinformatics* 2008;**24**:1547-8.

32 Teschendorff AE, Marabita F, Lechner M, Bartlett T, Tegner J, Gomez-Cabrero D, *et al.* A beta-mixture quantile normalization method for correcting probe design bias in Illumina Infinium 450 k DNA methylation data. *Bioinformatics* 2013;**29**:189-96.

33 Triche T Jr. IlluminaHumanMethylation450k.db: Illumina Human Methylation 450k annotation data. R package version 2.0.7 . 2015.

34 Szklarczyk D, Franceschini A, Wyder S, Forslund K, Heller D, Huerta-Cepas J, *et al.* STRING v10: proteinGÇôprotein interaction networks, integrated over the tree of life. *Nucleic Acids Research* 2015;**43**:D447-D452.

35 den Hollander W, Ramos YF, Bomer N, Elzinga S, van der Breggen R, Lakenberg N, *et al.* Transcriptional Associations of Osteoarthritis-Mediated Loss of Epigenetic Control in Articular Cartilage. *Arthritis Rheumatol* 2015;**67**:2108-16.

36 Livak KJ, Schmittgen TD. Analysis of Relative Gene Expression Data Using Real-Time Quantitative PCR and the 2GêÆ+ö+öCT Method. *Methods* 2001;**25**:402-8.

37 Toegel S, Huang W, Piana C, Unger F, Wirth M, Goldring M, *et al.* Selection of reliable reference genes for qPCR studies on chondroprotective action. *BMC Molecular Biology* 2007;**8**:13.

38 Fujii Y, Kitaura K, Matsutani T, Shirai K, Suzuki S, Takasaki T, *et al.* Immune-Related Gene Expression Profile in Laboratory Common Marmosets Assessed by an Accurate Quantitative Real-Time PCR Using Selected Reference Genes. *PLoS ONE* 2013;**8**:e56296.

39 Diederichs S, Tuan RS. Functional comparison of human-induced pluripotent stem cell-derived mesenchymal stem cells and bone marrow-derived mesenchymal stromal cells from the same donor. 23[14], 1594-1610. 2015. Stem cells and development.

40 Bell J, Pai A, Pickrell J, Gaffney D, Pique-Regi R, Degner J, *et al.* DNA methylation patterns associate with genetic and gene expression variation in HapMap cell lines. *Genome Biology* 2011;**12**:R10.

41 Zhang D, Cheng L, Badner JA, Chen C, Chen Q, Luo W, *et al.* Genetic Control of Individual Differences in Gene-Specific Methylation in Human Brain. *The American Journal of Human Genetics* 2010;**86**:411-9.

42 Gibbs JR, van der Brug MP, Hernandez DG, Traynor BJ, Nalls MA, Lai SL, *et al.* Abundant quantitative trait loci exist for DNA methylation and gene expression in human brain. *PLoS Genet* 2010;**6**:e1000952.

43 Wang Z, Kim JH, Higashino K, Kim SS, Wang S, Seki S, et al. Cartilage Intermediate Layer Protein (CILP) Regulation in Intervertebral Discs: The Effect of age, Degeneration, and Bone Morphogenetic Protein-2. 37[3], E203-E208. 2012. Spine.

44 Whittle M, Izeradjene K, Rani P, Feng L, Carlson M, DelGiorno K, *et al.* RUNX3 Controls a Metastatic Switch in Pancreatic Ductal Adenocarcinoma. *Cell* 2015;**161**:1345-60.

45 Liang Y, Hu J, Li J, Liu Y, Yu J, Zhuang X, *et al.* Epigenetic Activation of TWIST1 by MTDH Promotes Cancer Stem-like Cell Traits in Breast Cancer. *Cancer Research* 2015;**75**:3672-80.

46 Nagarajan RP, Zhang B, Bell RJA, Johnson BE, Olshen AB, Sundaram V, *et al.* Recurrent epimutations activate gene body promoters in primary glioblastoma. *Genome Research* 2014;**24**:761-74.

47 Martin V, Valencia A, Agirre X, Cervera J, Jose-Eneriz ES, Vilas-Zornoza A, *et al.* Epigenetic regulation of the non-canonical Wnt pathway in acute myeloid leukemia. *Cancer Science* 2010;**101**:425-32.

48 Yao L, Shen H, Laird P, Farnham P, Berman B. Inferring regulatory element landscapes and transcription factor networks from cancer methylomes. *Genome Biology* 2015;**16**:105.

49 Kim E, Kim M, Woo DH, Shin Y, Shin J, Chang N, *et al.* Phosphorylation of EZH2 Activates STAT3 Signaling via STAT3 Methylation and Promotes Tumorigenicity of Glioblastoma Stem-like Cells. *Cancer Cell* 2013;**23**:839-52.

50 Wyles CC, Houdek MT, Behfar A, Sierra RJ. Mesenchymal stem cell therapy for osteoarthritis: current perspectives. Stem Cells Cloning: Advances and Applications [8], 117-124. 2015. Stem Cells Cloning: Advances and Applications.

51 Barker N, Bartfeld S, Clevers H. Tissue-Resident Adult Stem Cell Populations of Rapidly Self-Renewing Organs. *Cell Stem Cell* 2010;**7**:656-70.